Unaerated feeding alters the fate of dissolved methane during aerobic wastewater treatment

Baeten, Janis E.; Walgraeve, Christophe; Granja, Rafael Cesar; van Loosdrecht, Mark C.M.; Volcke, Eveline I.P.

DOI
10.1016/j.watres.2021.117619

Publication date
2021

Document Version
Final published version

Published in
Water Research

Water Research 204 (2021) 117619

Contents lists available at ScienceDirect

Water Research

journal homepage: www.elsevier.com/locate/watres

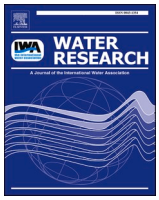

Unaerated feeding alters the fate of dissolved methane during aerobic wastewater treatment

Janis E. Baeten [a], Christophe Walgraeve [a], Rafael Cesar Granja [a], Mark C.M. van Loosdrecht [b], Eveline I.P. Volcke [a,*]

[a] Department of Green chemistry and Technology, Ghent University, Coupure Links 653, Ghent 9000, Belgium
[b] Department of Biotechnology, Delft University of Technology, Van der Maasweg 9, Delft 2629 HZ, the Netherlands

ARTICLE INFO

Keywords:
Methane oxidizing bacteria
Greenhouse gas
Wastewater treatment
Sequencing batch reactor
Emission
Aerobic granular sludge

ABSTRACT

In municipal wastewater treatment plants, some dissolved methane can enter the aerobic bioreactors. This greenhouse gas originates from sewers and return flows from anaerobic sludge treatment. In well-mixed conventional activated sludge reactors, methane emissions are largely avoided because methane oxidizing bacteria consume a large fraction, even without optimizing for this purpose. In this work, the fate of dissolved methane is studied in aerobic granular sludge reactors, as they become increasingly popular. The influence of the characteristic design and operating conditions of these reactors are studied with a mathematical model with apparent conversion kinetics and stripping: the separation of feeding and aeration in time, a higher substrate transport resistance, a high retention time of granular biomass and a taller water column. Even for a best-case scenario combining an unrealistically low intragranule substrate transport resistance, a high retention time, a tall reactor, an extremely high influent methane concentration and no oxygen limitation, the methane conversion efficiency was only 12% when feeding and aeration were separated in time, which is lower than for continuous activated sludge reactors under typical conditions. A more rigorous model was used to confirm the limited conversion, considering the multi-species and multi-substrate biofilm kinetics, anoxic methane consumers and the high substrate concentration at the bottom during upward plug flow feeding. The observed limited methane conversion is mainly due to the high concentration that accumulates during unaerated feeding phases, which favours stripping more than conversion in the subsequent aeration phase. Based on these findings, strategies were proposed to mitigate methane emissions from wastewater treatment plants with sequentially operated reactors.

1. Introduction

Methane (CH_4) emissions may account for 0 to 40% of the total carbon footprint of conventional, aerobic municipal wastewater treatment plants, but the exact value and hot-spots depend on the design and operation of a specific plant and sewer system (Foley et al., 2011; Masuda et al., 2018). Methane is produced during anaerobic conversions of organic material. This mainly occurs in sewers and sludge digesters, but can also take place in sludge thickeners and primary settlers (Daelman et al., 2012; Masuda et al., 2015). The average dissolved methane concentration in the influent ranges from 2 to 61 g COD.m^{-3} (Liu et al., 2015), depending on the residence time, geometry and type of sewers and on the wastewater characteristics and temperature (Foley et al., 2009; Short et al., 2017; Terryn et al., 2017). Dissolved methane can be stripped from several unit processes in a treatment plant. The headworks are a first source of emissions, accounting for 0 to 50% of the plant-wide emissions. The fraction that is stripped here increases if there is intense contact with air, e.g. when screw conveyors or aerated grit chambers are used (Daelman et al., 2012; Foley et al., 2011; Kwok et al., 2015; Liu et al., 2014; Masuda et al., 2018; Ren et al., 2013; Samuelsson et al., 2018; Wang et al., 2011). When present, primary settlers can also be a major emission source, with values ranging from less than 1 to 68% of the plant-wide emissions (Daelman et al., 2012; Liu et al., 2014; Masuda et al., 2018; Ren et al., 2013). The residual dissolved methane that reaches the bioreactors is nearly completely removed here, via stripping on the one hand and biological conversion (oxidation) on the other hand. Also the contribution of this unit process to the plant-wide methane emissions varies over a wide range, between 3 and 80% (Daelman et al., 2012; Kwok et al., 2015; Wang et al., 2011). Biological methane oxidation has been shown to remove 68–80% of the methane

* Corresponding author.
E-mail address: Eveline.Volcke@UGent.be (E.I.P. Volcke).

https://doi.org/10.1016/j.watres.2021.117619
Received 17 November 2020; Received in revised form 10 August 2021; Accepted 25 August 2021
Available online 28 August 2021

that enters continuous activated sludge reactors (Daelman et al., 2012; Liu et al., 2014). Methane emissions from a plant increase drastically if sludge is anaerobically digested. Methane can escape from the digesters directly, during sludge dewatering and storage and due to the incomplete combustion of biogas, which has been reported to sum up to 72-81 % of the plant-wide emissions (Daelman et al., 2012; Delre et al., 2017; Foley et al., 2011; Kwok et al., 2015; Samuelsson et al., 2018; Yoshida et al., 2014). Moreover, the reject water contains dissolved methane, which often enters the main treatment process again, where it can be emitted as mentioned above (Daelman et al., 2012; Ribera-Guardia et al., 2019). Literature thus clearly shows an immense variation of both the load and fate of methane between different plants. The potential hot-spots of methane input, production, emissions and conversion in wastewater treatment plants discussed in this section are summarized in Fig. 1.

The amount of methane oxidized in an activated sludge reactor depends on the design and operation. For example, there is an optimal aeration rate for methane oxidation, which is high enough to avoid oxygen limitations of the conversion, but low enough to avoid excessive stripping. Deeper diffusers also slightly improve conversions, as the hydraulic pressure improves the solubility of gases and therefore hinders methane stripping, while stimulating oxygen transfer. Finally, a continuously stirred tank reactor shows more conversion than a plug-flow type reactor because mixing dilutes the incoming methane, which decreases the stripping rate more than it decreases the conversion rate (Daelman et al., 2014). Notwithstanding these influencing factors, aerobic bioreactors are rarely or never optimized for methane conversion in municipal wastewater treatment plants, as COD and nutrient removal are the primary goals. Yet, even without optimization, measurements in continuous aerobic systems have always shown methane conversion efficiencies above 68% (Daelman et al., 2012; Liu et al., 2014). Besides, simulations under various conditions have consistently shown values above 21%, except when influent methane concentrations are below 5 g COD.m^{-3} (Daelman et al., 2014). This may give the impression that in cases where the influent methane concentration is high, aerobic methane conversion can always be relied on to mitigate the associated potential extra greenhouse gas emissions. However, it is not yet sure whether high methane conversion efficiencies are as easily achieved in sequentially operated reactors without aeration during the feeding phases. Sequential operation with unaerated feeding phases is becoming increasingly popular under the form of aerobic granular sludge reactors, which have lower space and energy requirements than conventional activated sludge systems (Pronk et al., 2017).

The fate of methane in aerobic granular sludge reactors has not yet been investigated. In these reactors, feeding and discharge are separated in time from aeration. Biomass is present in larger and denser aggregates than in conventional activated sludge reactors (Pronk et al., 2017). Granules have a higher resistance for substrate transport towards the microorganisms, leading to lower specific conversion rates at low limiting substrate concentrations (Baeten et al., 2018). At the same time, they have a higher solids retention time due to their excellent settleability (Ali et al., 2019; Winkler et al., 2012). Moreover, aerobic granular sludge reactors are typically taller (6–9 m) than conventional activated sludge reactors to enable feeding from the bottom while discharging effluent from the top via an upward plug flow (de Bruin et al., 2013). These characteristic design and operating conditions could influence the fate of methane entering these reactors in different ways. From earlier work, one can deduce that the higher mass transport resistance may limit conversion (Baeten et al., 2018), the discontinuous feeding may promote stripping (Mozo et al., 2012), the higher solids retention time may promote conversion (Henze et al., 2008) and the taller reactor height may limit stripping (Daelman et al., 2014). Yet, the magnitude of these effects for the typical design and operating conditions of aerobic granular sludge reactors and their combined effect remain difficult to predict. As the fate of methane could be altered, these reactor types may also require different strategies to minimize emissions.

This work investigates for the first time the fate of dissolved methane entering sequentially operated reactors with unaerated feeding phases in general, and aerobic granular sludge reactors in particular. First, a simple mass balance model for the fate of methane and Methane Oxidizing Bacteria (MOB) was set-up and used to separately investigate the effects of separating feeding and aeration in time (i.e. sequential versus continuous reactor operation), more intragranule transport resistance, higher solids retention times and increased reactor heights. A more rigorous model was then developed to confirm the results for the best-case scenario, considering the multi-species and multi-substrate biofilm kinetics, presence of anoxic methane oxidizers and the high substrate concentration at the bottom during the upward plug flow during feeding.

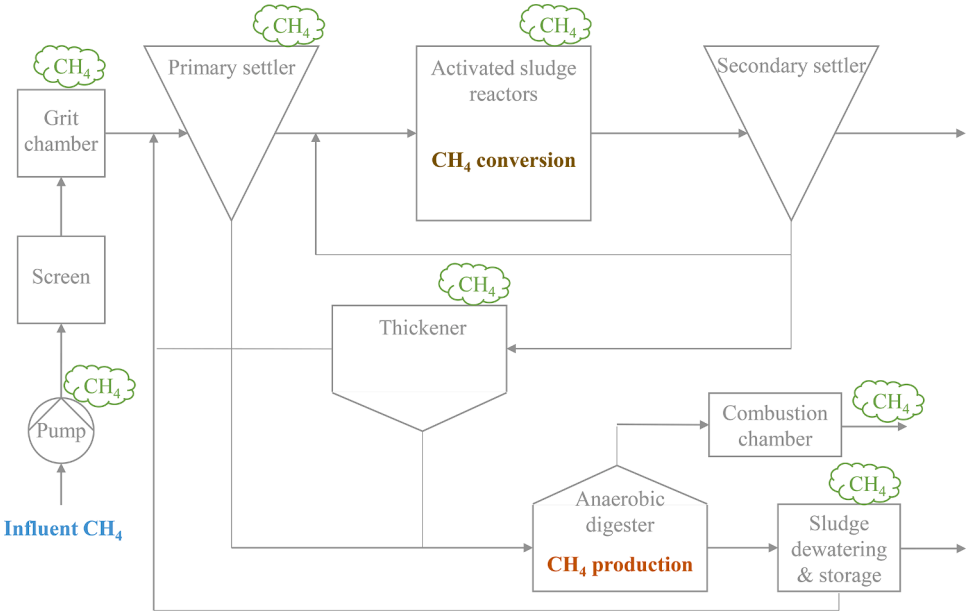

Fig. 1. Typical hot-spots of methane input, production, emission and conversion (biological oxidation) in a wastewater treatment plant, indicated with green clouds.

2. Methodology

2.1. Influence of design and operating conditions

A mathematical model was set up to study how the methane conversion efficiency is affected by sequential feeding and aeration, a higher intragranule substrate transport resistance, a higher solids retention time and taller reactors. First, a general mass balance was set up for methane (2.1.1) and methane oxidizing bacteria (2.1.2). Then, the simulated scenarios were defined for a sequentially (2.1.3) and continuously operated reactor (2.1.4) to investigate the effect of separating feeding and aeration in time. The other design and operating conditions were kept the same for a fair comparison: the volumetric overall transfer coefficient of oxygen, average influent flow rate, solids retention time of methane oxidizing bacteria, reactor height, conversion kinetics and stoichiometry and aerobic hydraulic retention time. All applied parameter values are summarized in Table 1. MATLAB scripts are available as supplementary information.

2.1.1. Methane mass balance

A mass balance for dissolved methane, m_{CH4} (g COD), was set up for a completely mixed reactor, considering the reactor influent as the sole source of methane and the effluent, stripping and biological conversion as sinks (Eq. (1); Fig. 2).

$$\frac{dm_{CH4}(t)}{dt} = Q_{in}(t)S_{CH4,in}(t) - Q_{out}(t)S_{CH4}(t) - \dot{m}^{L-G}_{CH4}(t) - \dot{R}_{CH4}(t) \quad (1)$$

Q_{in} and Q_{out} ($m^3.d^{-1}$) are the imposed liquid flows, respectively into and out of the reactor, $S_{CH4,in}$ and S_{CH4} (g COD.m^{-3}) the respective incoming and outgoing methane concentration, $m^{L\text{-}G}_{CH4}$ (g COD.d^{-1}) the stripping rate and R_{CH4} (g COD.d^{-1}) the conversion rate. The concentration of methane in the liquid volume V (m^3) relates to its total mass via Eq. (2).

$$S_{CH4}(t) = \frac{m_{CH4}(t)}{V(t)} \quad (2)$$

The stripping rate was described with a liquid-gas transfer model (Eq. (3)) that considers the mean gas phase mole fraction and mean pressure along the reactor height (Baeten et al., 2020).

$$\dot{m}^{L-G}_{CH4}(t) = K_L a_{O2}(t)V(t)\frac{S_{CH4}(t) - i_{COD,CH4}h_{CH4}\frac{\left(p^G_{atm}+\rho g\frac{H}{2}\right)M_{CH4}}{RT}x^G_{in,CH4}}{\sqrt{\frac{D_{O2}}{D_{CH4}}}+0.6h_{CH4}\frac{H}{2}} \quad (3)$$

K_La_{O2} (d^{-1}) denotes the volumetric overall transfer coefficient of oxygen, $i_{COD,CH4}$ (g COD.g^{-1}) the COD content of methane, h_{CH4} (g.m^{-3} in the liquid phase per g.m^{-3} in the gas phase) the Henry coefficient of methane, p^G_{atm} (Pa) the atmospheric pressure, ρ (kg.m^{-3}) the density of water, g (m.s^{-2}) the gravitational acceleration, H (m) the water column height during aeration, M_{CH4} (g.$mole^{-1}$) the molecular mass of methane, R (J.$mole^{-1}$.K^{-1}) the universal gas constant, T the reactor temperature (K), $x^G_{in,CH4}$ (mole.$mole^{-1}$) the mole fraction of methane in the atmosphere and D_{O2} and D_{CH4} (m^2.d^{-1}) are the respective diffusion coefficients of oxygen and methane.

The conversion rate was calculated based on the stoichiometry and kinetics for methane oxidizing bacteria reported by Arcangeli and Arvin (1999) (Eq. (4)).

$$\dot{R}_{CH4}(t) = \frac{\mu_{MOB,Max}(t)}{Y_{MOB}}\frac{S_{CH4}}{S_{CH4}+K_{CH4,MOB}}X_{MOB}(t)V(t) \quad (4)$$

Table 1
Parameters used for the simple model.

Parameter	Symbol	Reference value (applied range)	Unit	Refs. or explanation
Physical, chemical and biological parameters				
Universal gas constant	R	8.31	J.$mole^{-1}$.K^{-1}	Çengel et al. (2012)
Gravitational acceleration	g	9.81	m.s^{-2}	Çengel et al. (2012)
Density of water	ρ	1000	kg.m^{-3}	Çengel et al. (2012)
Atmospheric pressure	p^G_{atm}	101325	Pa	Çengel et al. (2012)
Temperature	T	293.15	K	Pronk et al. (2015)
Diffusion coefficient of oxygen at 20°C	D_{O2}	1.83	10^{-4} m^2.d^{-1}	Gmehling et al. (2010)
Diffusion coefficient of methane at 20°	D_{CH4}	1.39	10^{-4} m^2.d^{-1}	Gmehling et al. (2010)
Henry coefficient of methane at 20°	h_{CH4}	0.0351	g.m^{-3}/(g.m^{-3}) (liquid/gas)	Sander (2015)
Molecular mass of methane	M_{CH4}	16	g.$mole^{-1}$	Meija et al. (2016); Sander (2015)
Mole fraction of methane in the atmosphere	$x^G_{in,CH4}$	0.0000018	mole.$mole^{-1}$	Abalakin (2010)
COD content of methane	$i_{COD,CH4}$	4	g COD.g^{-1}	Henze et al. (2008)
MOB yield	Y_{MOB}	0.2	g COD. g COD^{-1}	Arcangeli and Arvin (1999)
MOB maximal specific growth rate at 20°C	$\mu_{MOB,Max}$	1.6	d^{-1}	Arcangeli and Arvin (1999)
MOB specific decay rate at 20°C	b_{MOB}	0.24	d^{-1}	Arcangeli and Arvin (1999)
MOB apparent half-saturation coefficient	$K_{CH4,MOB}$	0.26 (0.04-2)	g COD.m^{-3}	Arcangeli and Arvin (1999)
Reactor design and operation				
Influent methane concentration	$S_{CH4,in}$	21 (2 – 61)	g COD.m^{-3}	Median (Liu et al., 2015)
Volumetric overall transfer coefficient of oxygen during aeration	K_La_{O2}	100	d^{-1}	Limited oxygen limitation (Daelman et al., 2014)
Solids retention time of MOB	SRT_{MOB}	29 (1-150)	d	Pronk et al. (2015) and Ali et al. (2019)
Average influent flow rate	Q	14300	m^3.d^{-1}	Pronk et al. (2015)
Water column height	H	7.5 (2-12)	m	Pronk et al. (2015)
Maximal volume for sequential operation	$V_{seq,max}$	9600	m^3	Pronk et al. (2015)
Feeding time	$T_{feeding}$	1	h	Pronk et al. (2015)
Aeration time	$T_{aeration}$	5	h	Pronk et al. (2015)
Settling time	$T_{settling}$	20	min	Pronk et al. (2015)
Discharge time	$T_{discharge}$	10	min	Assumed
Initial conditions				
Initial MOB concentration	$X_{MOB,ini}$	10	g COD.m^{-3}	Daelman et al. (2014)
Initial methane concentration	$S_{CH4,ini}$	0	g COD.m^{-3}	Assumed

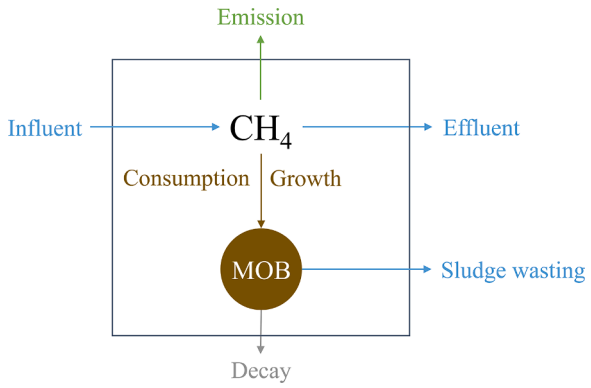

Fig. 2. Sinks and sources of methane (CH_4) and methane oxidizing bacteria (MOB) considered in the simple model.

$\mu_{MOB,Max}$ (d^{-1}) is the maximal specific growth rate of MOB, Y_{MOB} (g COD.g COD^{-1}) their yield, $K_{CH4,MOB}$ (g COD.m^{-3}) the apparent half-saturation coefficient for methane and X_{MOB} (g COD) the biomass concentration. The Monod term for oxygen was omitted in Eq. (4) to represent an optimistic scenario, without oxygen limitation. For activated sludge, it has been shown that oxygen limitations are small for a K_La_{O2} above 80 d^{-1} (Daelman et al., 2014). For granular sludge, this optimistic assumption may overestimate the predicted conversion rates more, as specific conversion rates are lower for the same oxygen concentration when biomass is present in dense aggregates. Also for sequential reactor operation, neglecting oxygen limitation overestimates conversion rates more, as the high ammonium and organics concentrations after feeding cause stronger competition for oxygen from nitrifiers and heterotrophs. Only the half-saturation coefficient for methane $K_{CH4,MOB}$ (g COD.m^{-3}) was varied to represent the difference between flocculent (low $K_{CH4,MOB}$) and granular sludge (high $K_{CH4,MOB}$) (Baeten et al., 2018).

2.1.2. Methane oxidizing bacteria mass balance

The mass balance of methane oxidizing bacteria m_{MOB} (g COD) considered growth as the sole source and decay and sludge wasting as sinks (Eq. (5); Fig. 2).

$$\frac{dm_{MOB}(t)}{dt} = Y_{MOB}\dot{R}_{CH4}(t) - b_{MOB}X_{MOB}(t)V(t) - d_{MOB}(t)X_{MOB}(t)V(t) \quad (5)$$

The first term on the right side, the growth rate, was considered directly coupled to the methane conversion rate $\dot{R}_{CH4}$ (Eq. (4)) via the yield Y_{MOB} (g COD.g COD^{-1}). The second term, the decay rate, was calculated via the specific decay rate, b_{MOB} (d^{-1}). The last term, the sludge wasting rate, was calculated via a specific waste rate d_{MOB} (d^{-1}), which is defined separately for the sequentially and continuously operated reactor below. The concentration of methane in the liquid volume V (m^3) relates to its total mass via Eq. (6).

$$X_{MOB}(t) = \frac{m_{MOB}(t)}{V(t)} \quad (6)$$

2.1.3. Solution for a sequentially operated reactor

The design and operating parameters were based on a full-scale aerobic granular sludge plant described in literature (Pronk et al., 2015) to have a realistic hydraulic retention time, average solids retention time and duration of the feeding and aeration phase (Table 1). The parameters Q_{in}, Q_{out}, K_La_{O2}, $\mu_{MOB,Max}$ and d_{MOB} were defined as periodic functions of time to represent sequential feeding, aeration, settling and simultaneous discharge and waste phases (Fig. 3). Discharge was considered separated from feeding, as in conventional sequencing batch reactors (Artan and Orhon, 2005). The flow rates during feeding and discharge were defined to treat the complete average influent flow rate Q ($m^3.d^{-1}$). K_La_{O2} and $\mu_{MOB,Max}$ were set to zero outside of aeration phases, to avoid stripping and conversions. The specific waste rate was defined to obtain the anticipated SRT of methane oxidizing bacteria, SRT_{MOB} (d).

The mass balances (Eqs. (1) and (5)) were solved for the steady state mass of methane m_{CH4} and methane oxidizing bacteria m_{MOB} in MATLAB, using the ODE15s algorithm. For some simulations, only the methane mass balance (Eq. (1)) was solved, with a fixed MOB population. Steady state was considered after 2000 cycles if MOB dynamics were included and after 10 cycles with a fixed MOB population. The last

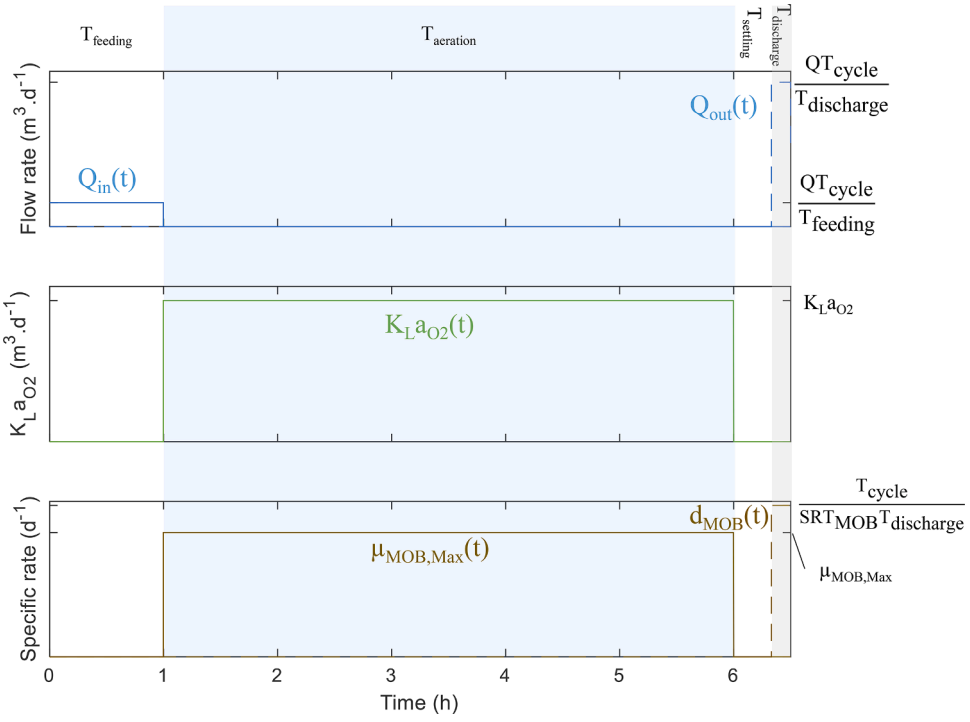

Fig. 3. Periodic variation of the parameters Q^L_{in}, Q^L_{out}, K_La_{O2}, $\mu_{MOB,Max}$ and d_{MOB} during one cycle of a sequentially operated reactor.

simulated cycle was always used to calculate the total amounts of methane lost via the effluent, consumed by MOB and emitted to the atmosphere.

2.1.4. Solution for a continuously operated reactor

The same aerobic hydraulic retention time as for sequential operation was obtained by using a slightly lower reactor volume V_{cont} (m^3) defined by Eq. (7), to compensate for the unaerated periods without stripping or conversion.

$$V_{cont} = \frac{T_{aeration} V_{seq,max}}{T_{cycle}} \quad (7)$$

The specific waste rate was defined with Eq. (8) to obtain the same SRT_{MOB}.

$$\dot{m}^{sludge}_{out,MOB}(t) = \frac{m_{MOB}(t)}{SRT_{MOB}} \quad (8)$$

For a continuously operated reactor, the mass balances (Eqs. (1) and (5)) were solved analytically (Supplementary Information Section S1) for the steady state mass of methane $m_{CH4,SS}$ and methane oxidizing bacteria $m_{MOB,SS}$.

2.2. Confirmation with a rigorous biofilm model

A more rigorous model was applied to verify the methane conversion efficiency predicted for a sequentially operated reactor in the best-case scenario. It considered the multi-species and multi-substrate biofilm kinetics, anoxic methane consumers and higher substrate concentrations in the granule bed during upward plug flow during feeding, which were neglected in the simple model described above. A summary is given here, while details on the implementation and parameter values are provided in supplementary information (Section S2 and Aquasim file).

2.2.1. Biological conversions

Not only aerobic methane consumption by Methane Oxidizing Bacteria (MOB), but also anoxic consumption by Denitrifying Anaerobic Methane Oxidizing Archaea (DAMOA) and Denitrifying Anaerobic Methane Oxidizing Bacteria (DAMOB) were described with stoichiometry and kinetics from literature (Arcangeli and Arvin, 1999; Chen et al., 2014; Lopes et al., 2011). For the half-saturation coefficients for methane, the value from the best-case scenario (0.04 g $COD.m^{-3}$) was applied for all methane oxidizing groups, which is 147 times smaller than reported for DAMOA and DAMOB (Chen et al., 2014). Monod and inhibition terms for oxygen were included here, in contrast to the simplified approach used before (Eq. (2)), to account for the competition for oxygen with other microbial groups. The conversions catalysed by ordinary heterotrophic organisms, phosphate accumulating organisms, ammonium oxidizing organisms and nitrite oxidizing organisms were described with ASM2d (Henze et al., 2000) as corrected by Hauduc et al., (2010) and extended with two-step nitrification (Sin et al., 2008) and first order hydrolysis kinetics (Baeten et al., 2019; Vanrolleghem et al., 2003).

2.2.2. Mass transport and transfer

The model was set up in Aquasim (Reichert, 1994), comprising a dynamic 1D biofilm model, which calculates the microbial population distribution over the granule depth resulting from competition for space and substrates (Wanner and Gujer, 1986). The same reactor design and operation was applied as in the simple model for a sequentially operated reactor, but additional parameters were required here. The influent composition in terms of COD, N and P was based on values for the reference reactor (Pronk et al., 2015) and a typical fractionation in The Netherlands (Roeleveld and van Loosdrecht, 2002). A high influent methane concentration was used to represent a best-case scenario ($S_{CH4,in}$ = 61 g $COD.m^{-3}$).

The total reactor volume was split up into a 1100 m^3 biofilm compartment, which represents the settled sludge bed at the bottom of the reactor, and a mixed compartment (8500 m^3 after feeding), which represents the top part of the reactor (Fig. 4). During feeding, the diffusive exchange coefficient between the two compartments was set to zero to obtain a higher concentration of substrates in the sludge bed than in the rest of the reactor, as in a full-scale reactor during upward plug flow feeding (Pronk et al., 2015). During other phases, the exchange coefficient was increased to let the liquid phases of both compartments behave as one mixed, fluctuating water volume without numerical errors (Baeten et al., 2021). A tall reactor (H = 12 m) was assumed to calculate the liquid-gas transfer rate of methane (Eq. (3)) and oxygen (Eq. (S10)), to represent a best-case scenario. The simulated aeration control strategy was based on the full-scale operation, using a fixed dissolved oxygen set-point during the aeration phases, until the ammonium concentration drops below its set-point (Pronk et al., 2015). The applied granule size was based on measurements on full-scale (van Dijk et al., 2018) and the granule depth was divided into 20 grid points. Mass transfer resistance from the bulk liquid to the granule surface was neglected. 750 days were simulated.

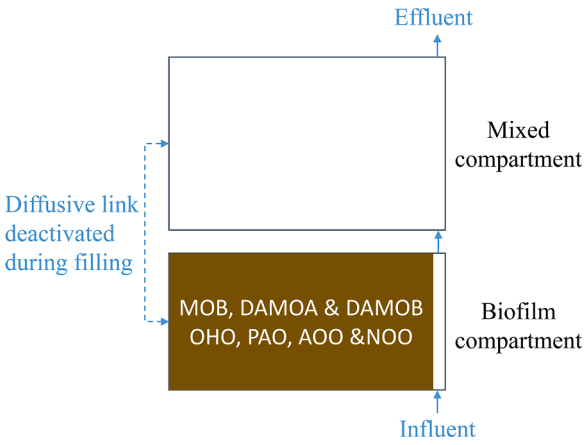

Fig. 4. Representation of the multi-species and multi-substrate biofilm kinetics, anoxic methane consumers and high substrate concentrations in the settled sludge bed during upward plug flow feeding in the rigorous model.

3. Results and discussion

3.1. Influence of design and operating conditions

First, the fate of influent methane simulated with the simple model was compared between a continuously and sequentially operated reactor (3.1.1) for the reference parameter values (Table 1) to assess the effect of separating feeding and aeration, which is used in some sequencing batch reactors with flocculent sludge and in full-scale aerobic granular sludge reactors. Then, the effect of different design and operating conditions was studied (3.1.2–3.1.5).

	Sink of methane	Continuous	Sequential
Fixed MOB population	% converted	70	24
	% emitted	29	76
	% to the effluent	1	0
Dynamic MOB population	% converted	88	0
	% emitted	12	100
	% to the effluent	0	0

Fig. 5. Fate of methane for the reference case parameters (Table 1) in case of a fixed population size of methane oxidizing bacteria (X_{MOB} = 10 g $COD.m^{-3}$ during the aeration phase) or dynamic population in a continuously or sequentially operated reactor, respectively.

3.1.1. Unaerated feeding (reference case)

Conversion was the main sink of methane (70%) when a continuously operated reactor was simulated with a fixed, typical concentration of methane oxidizing bacteria of 10 g COD.m^{-3}, while the contribution of the effluent load was negligible (Fig. 5). Both results are in line with the experimental findings of Daelman et al. (2012) and Liu et al. (2014). In contrast, sequential operation with the same fixed population size of methane oxidizing bacteria led to significantly less conversion (24%) and more stripping (76%). The lower predicted conversion efficiency was due to the separation of feeding and aeration in time, as this was the only difference between the two scenarios.

The cyclic dynamics of the sequentially operated reactor give insight in the cause of the higher emissions. During feeding (Fig. 6C), no conversion or stripping occurred (Fig. 6A), while methane entered via the influent, which led to methane accumulation in the liquid phase. This resulted in a high dissolved methane concentration at the beginning of the aeration phase (Fig. 6B). Upon the start of aeration, the emission rate was higher than the conversion rate (Fig. 6A). This is because the stripping rate increases linearly with the methane concentration, while the conversion rate saturates towards a maximal value (Fig. 7). Only when the methane concentration dropped below 0.72 g COD.m^{-3} did the stripping rate drop below the conversion rate. However, by this time, most of the methane had already been emitted. Experimental off-gas

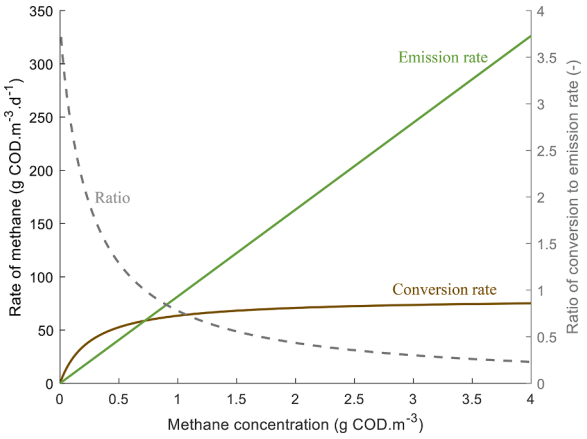

Fig. 7. Emission and conversion rate and their respective ratio as a function of the dissolved methane concentration for an apparent half-saturation coefficient $K_{CH4,MOB}$ = 0.26 g COD.m^{-3}, concentration of methane oxidizing bacteria X_{MOB} = 10 g COD.m^{-3} and volumetric overall transfer coefficient of oxygen K_La_{O2} = 100 d^{-1}, simulated with the simple model.

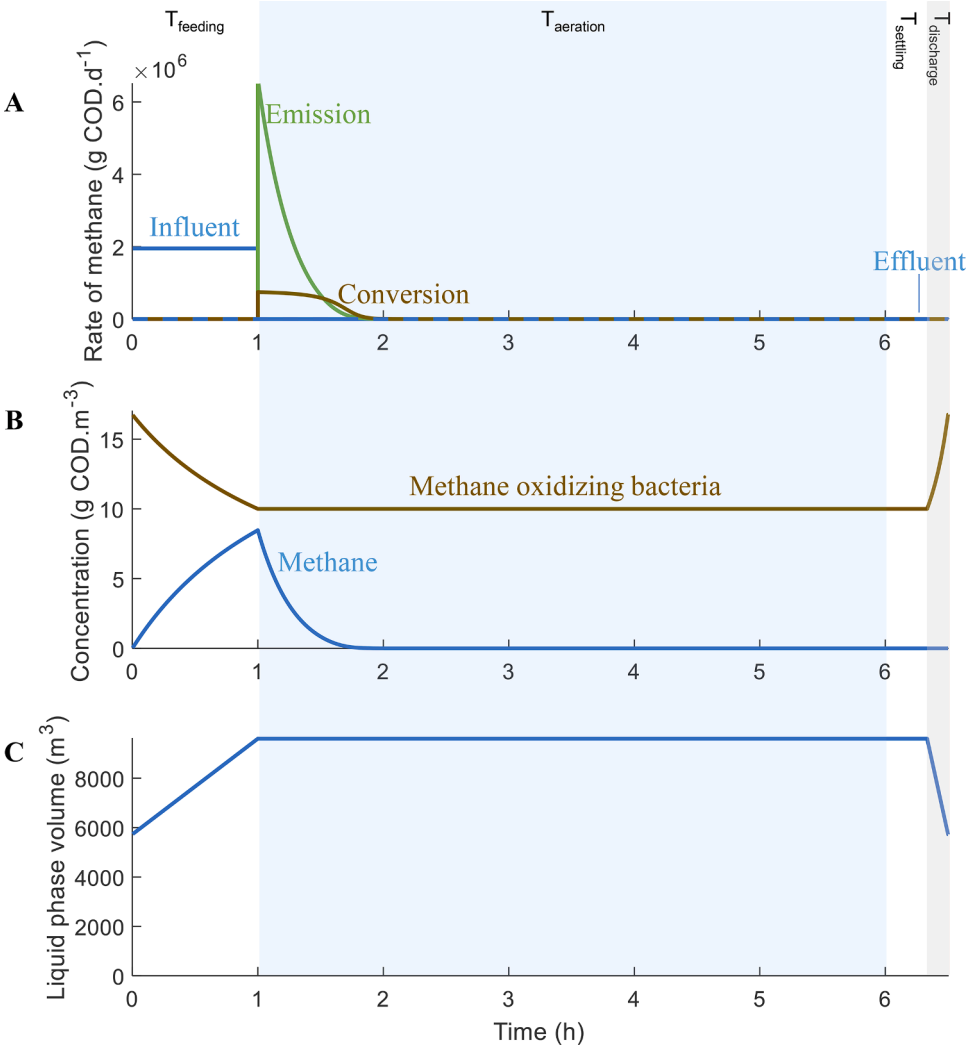

Fig. 6. Cyclic changes in a sequentially operated reactor with a fixed amount of biomass (X_{MOB} = 10 g COD.m^{-3} during the aeration phase) simulated with the simple model. (A) Rate of methane input, emission, conversion and output. (B) Concentration of methane and methane oxidizing bacteria. (C) Mixed liquor volume in the reactor. All parameters were set at their reference value (Table 1).

analyzes on aerobic granular sludge reactors have similarly shown a rapid decrease of the emission rate within the first 2 h of aeration (Baeten et al., In press; de Bruin et al. 2013). Conversely, the steady state methane concentration in a continuously operated reactor was low (0.14 g COD.m^{-3}) due to the constant dilution, conversion and stripping. This constantly low concentration favours conversion over stripping (Fig. 7). It can be concluded that a separate, unaerated feeding phase lowers the overall conversion efficiency because methane accumulates during feeding, which favours stripping.

When biomass dynamics were considered, the difference between the continuous and sequential operation became more pronounced: even more methane conversion was predicted for the continuous operation (88%) and no conversion at all was seen for the sequential operation (Fig. 5). As a larger fraction of the influent methane was stripped during sequential operation, the methane available for growth of methane oxidizing bacteria was insufficient to compensate the loss via decay and wasting. Consequently, the amount of biomass decreased during consecutive cycles, causing a lower methane conversion efficiency in turn. A critical amount of methane conversion is necessary to maintain a population of methane oxidizing organisms, which was not achieved in the reference sequentially operated reactor.

3.1.2. Higher intragranule transport resistance ($K_{CH4,MOB}$)

For a fixed population of methane oxidizing bacteria, more intragranule transport resistance (higher $K_{CH4,CH4}$, representing a higher degree of biomass aggregation) resulted in less methane conversion and thus more stripping, both for continuous and sequentially operated reactors (Fig. 8). This can be explained by the lower conversion rates, due to the occurrence of $K_{CH4,MOB}$ of in the denominator of the Monod expression (Eq. (4)). The conversion efficiency was always larger for continuous than for sequential operation. When microbial dynamics were included, this difference became even bigger, over the complete anticipated range of apparent half-saturation coefficients. An active population of methane oxidizers was always maintained during continuous operation. Consequently, aerobic methane oxidation is always expected to some extent in continuously operated reactors with enough oxygen supply, even if the biomass is granular (Kent et al., 2018; Wei et al., 2020). With sequential operation on the other hand, wash-out already occurred when $K_{CH4,MOB}$ was above 0.2 g COD.m^{-3}, which is on the low end of the range of experimentally observed values (Arcangeli and Arvin, 1999) and is therefore more representative for suspended cells or small flocs than for granules. Even for the lowest reported $K_{CH4,MOB}$ (0.04 g COD.m^{-3}, which practically results in zero order kinetics), only 7% was converted. So even for a sequentially operated reactor with flocculent sludge (Kuba et al., 1993), the population of methane oxidizing bacteria is expected to be smaller than for a continuously operated reactor with otherwise similar design and operating conditions.

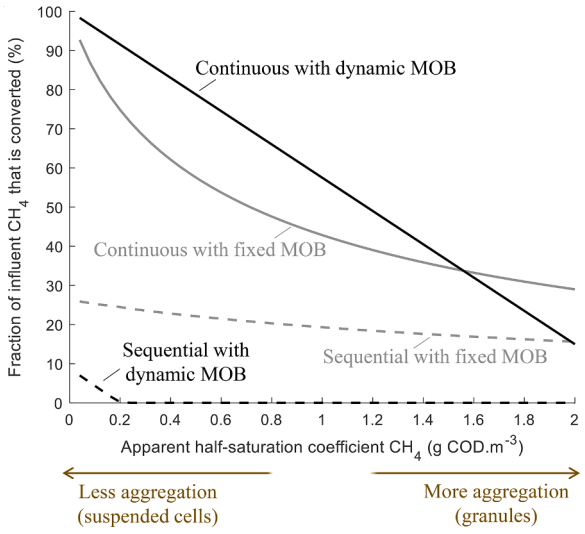

Fig. 8. Effect of the apparent half-saturation coefficient of methane $K_{CH4,MOB}$ on the methane conversion efficiency simulated with the simple model. The range of $K_{CH4,MOB}$ values reflects the anticipated range from suspended cells over flocs to granules (Arcangeli and Arvin, 1999). All other parameters were set at their reference value (Table 1).

3.1.3. Higher biomass retention

For a continuously operated reactor, a higher retention time led to more methane conversion, but it saturated quickly (Fig. 9). The population size and thus also the conversion efficiency increased sensitively with an increasing SRT_{MOB} up to 4 days, because wasting of methane oxidizers was slower (Eq. (8)). Afterwards, the impact on the population size diminished because the waste rate became smaller than the decay rate (Eq. (5)), which is unaffected by the SRT_{MOB}. For sequential operation, a slight improvement of the methane conversion was also observed with increasing SRT_{MOB}. However, it did not exceed 1.4%, even at an SRT_{MOB} of 150 days, which is representative for large granules in a full-scale plant (Ali et al., 2019). Consequently, the better retention of granules cannot compensate for the decrease of the methane oxidation efficiency resulting from sequential operation.

3.1.4. Taller reactors

For continuous operation, a higher reactor led to a slightly more methane conversion () under the given assumptions. This can be explained by the increased solubility of methane due to the higher hydraulic pressure, which decreases the stripping rate (Eq. (3)). However, this effect is marginal due to the low Henry coefficient and negligible content of methane in air (Baeten et al., 2020). Daelman et al. (2012) did predict a significant improvement, but mainly due to the improved absorption of oxygen, which has a much higher concentration in the air (20.946%). In the simple model applied in this work, oxygen limitation was already neglected altogether, as an optimistic scenario. Due to the minor effect of the reactor height on the stripping rate, wash-out of methane oxidizers could not be prevented during sequential operation, even with a 12 m tall reactor. As oxygen limitation was neglected, this does not prove that a taller reactor can never improve the methane conversion efficiency, but it does show the upper limit of this effect, which is apparently far less strong than the negative effect of an unaerated feeding phase.

3.1.5. Higher influent methane concentration (best-case scenario)

As the detrimental effect of sequential operation on the methane conversion efficiency could not be countered with less intragranule transport resistance, better biomass retention nor by taller reactors, this section explores whether the combined effects of the most beneficial design and operating conditions could: a low apparent half-saturation (representative for small flocs), a high solids retention time (representative for large granules), a tall reactor (even higher than typical granular sludge reactors) and increased influent methane concentrations (the highest average reported), still without any oxygen limitation represents (Fig. 9). A higher influent methane concentration increased the percentage conversion, as predicted by Daelman et al. (2014) for activated sludge systems. However, even for the best-case scenario, with the highest average influent concentration reported ($S^{L}_{in,CH4}$ = 61 g COD.m^{-3}), the conversion efficiency was no more than 12% during sequential operation, while nearly 100% methane conversion was found during continuous operation. With more realistic assumptions, including oxygen limitation and a higher transport resistance, and more moderate conditions, meaning lower influent methane concentrations and less tall reactors, even less aerobic methane oxidation will occur than predicted. A one-at-a-time sensitivity analysis for this best-case scenario showed that the specific growth and decay rate were the most sensitive biological parameters (Fig. S2). Sequential operation still led to less methane

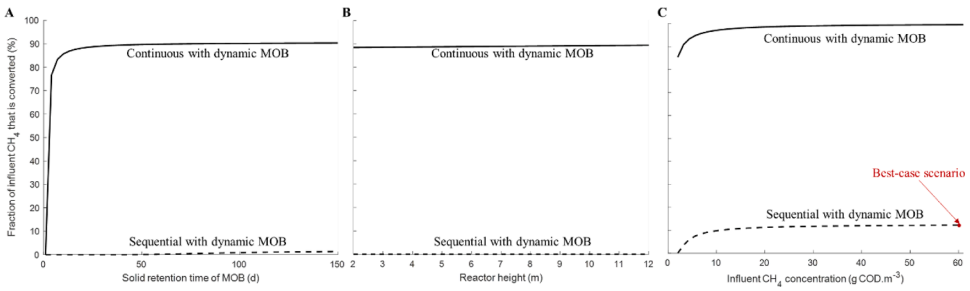

Fig. 9. The effect of (A) the retention time of methane oxidizing bacteria, (B) the reactor height and (C) the influent methane concentration on the methane conversion efficiency simulated with the simple model. (A) The range of SRT_{MOB} values reflects the anticipated range from suspended cells over flocs to granules (Ali et al., 2019). All other parameters were set at their reference value (Table 1). (B) The range of reactor heights covers most aerobic wastewater reactor designs. All other parameters were set at their reference value. (C) A low apparent half-saturation coefficient ($K_{CH4,MOB}$ = 0.04 g $COD.m^{-3}$), high solid retention time (SRT_{MOB} = 150 d) and tall reactor (H = 12 m) were used to obtain a best-case scenario at the highest influent concentration, while all other parameters were set at their reference value.

conversion than continuous operation over the complete range of values found in literature. Even for the outlier parameter values, methane conversion stayed below the reference value of 88% for the continuous operation (Fig. 5). For example, 81% was found for $\mu_{MOB,Max}$ = 12.9 d^{-1} (8 times the reference value), but this extremely high growth rate actually co-occurred with an extremely high decay coefficient b_{MOB} = 0.96 d^{-1} (Arcangeli and Arvin, 1999). This would again diminish the conversion efficiency, but this is not reflected in a one-at-a-time sensitivity analysis.

3.2. Confirmation with a rigorous biofilm model

Even though the simple model predicts that stripping is the main fate of methane in a sequentially operated reactor for the best-case scenario in terms of design, operation and biological parameters, two mechanisms were neglected which may lead to higher values. First, apparent kinetics may have underestimated the conversion because part of the methane will have diffused inside the granules during the unaerated feeding phase. The upward plug flow through the settled sludge bed would even lead to more methane entering the granules, as the incoming methane is not diluted with the rest of the reactor contents until aeration starts. This fraction of methane inside the granules does not experience the diffusional resistance for conversion. Secondly, anoxic methane consumers might be able to survive, using nitrate and nitrite instead of oxygen as electron acceptor. To account for these possibilities, the best-case scenario was also simulated with a multi-species and multi-substrate biofilm model, including anoxic methane consumers and the concentrated methane in the granule bed during upward plug flow feeding.

The simulation with the rigorous model showed only 7% methane conversion after 750 days of simulation, which is even lower than predicted by the simple model (Fig. 9). As expected, there was a flux of methane into the granules during feeding (Fig. 10A). When aeration started, mixing between the water at the top and bottom led to a sudden drop of the methane concentration in the sludge bed (Fig. 10C), causing a negative peak in the diffusive flux, i.e. out of the granules. This led to a fast decrease of intragranule methane concentration profiles (Fig. S6). The stripping peak (Fig. 10C) occurred only 1 min after the peak of the outward flux. This indicates that neglecting diffusion (as in the simple model) does not significantly underestimate the conversions after all, due to fast diffusion kinetics. Aerobic methane oxidizing bacteria almost completely washed out (Fig. S3). This can be explained by the competition for oxygen by heterotrophs and nitrifiers, which was now included (Tables S2 and S4 and Fig. S5). On the other hand, anoxic methane consumers were maintained in the system. DAMOB, which use nitrite, were most abundant and resided primarily in the inner layers of the granule (Fig. S4), which is explained by their inhibition by oxygen in the outer layers (Table S4). The DAMOA population did not yet reach a steady state after 750 days of simulation. Even with an active population of anoxic methane consumers, the majority of the influent methane is

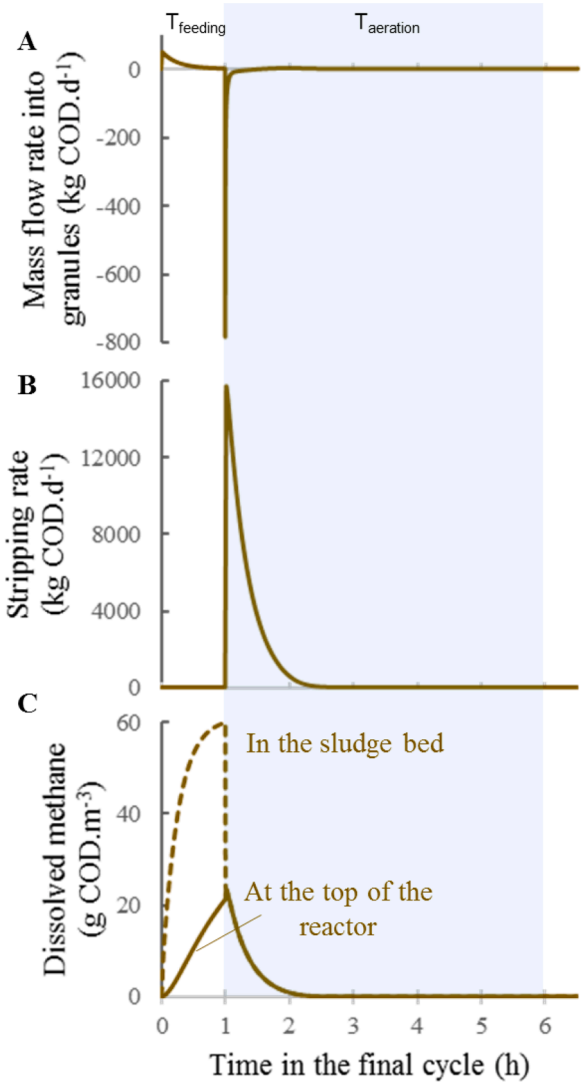

Fig. 10. Mass flow rate into the granules (A), stripping rate (B) and liquid phase concentration of methane (C) simulated with the rigorous biofilm model for a cycle after 750 days operation of a sequentially operated reactor for a best-case scenario: low apparent half-saturation coefficients ($K_{CH4,MOB}$ = $K_{CH4,DAMOA}$ = $K_{CH4,DAMOB}$ = 0.04 g $COD.m^{-3}$), a tall reactor (H = 12 m) and high influent methane concentration ($S_{CH4,in}$ = 61 g $COD.m^{-3}$).

still stripped, so only a fraction could be used as an electron donor for denitrification.

The same conclusion was reached as with the simple model: low methane conversion efficiencies are expected in sequentially operated aerobic granular sludge reactors. However, it took more than 5000 times longer to perform one simulation (2 min versus more than a week). This shows the strength of the simple model: it is easier to understand and it allows scanning the parameter space to study the effect of different parameters within a reasonable timeframe. Yet the benefit of the rigorous model was that it could be used to verify whether the conclusion derived from the simple model was robust for the simplifying assumptions that were made.

There are still a few mechanisms which were not modeled and which might lead to higher methane conversion efficiencies. Some studies have shown methanotrophic activity of nitrifiers (Daebeler et al., 2014; Jones and Morita, 1983; Ward, 1987) and nitrifying activity of methanotrophs (O'Neill and Wilkinson, 1977; Yoshinari, 1985). If the nitrifiers were able to convert a significant fraction of methane, a certain amount of methane conversion capacity could be maintained, as the nitrifiers have ample ammonium as substrate. Conversely, if the methanotrophs are able to grow on ammonium, also some conversion capacity can be maintained. However, these effects are probably limited due to competitive inhibition of ammonium on the methane oxidation rate (King and Schnell, 1994; Nyerges and Stein, 2009), especially as sequential operation leads to accumulation of ammonium during an unaerated feeding phase, intensifying the competitive inhibition. Moreover, immigration of methane consumers may also occur from the sewers. The effect of temperature was not included in this study because the wastewater temperature is not expected to be significantly different between continuous and sequentially operated reactors and is therefore out of scope.

3.3. Implications for limiting greenhouse gas emissions

There is a range of operating conditions between a sequentially operated reactor with an unaerated feeding phase and a reactor with continuous feeding and aeration. For example, a sequentially operated reactor can have an aerated feeding phase (Artan and Orhon, 2005). In this case, the dissolved methane concentration is kept lower during feeding due to the conversion and stripping that are favoured by the still active aeration, which would favour conversion (Fig. 7). Liu et al. (2014) found 48% methane conversion in a full-scale reactor with such sequential operation with aerobic feeding. This is lower than the efficiencies found for continuously fed and aerated reactors (Daelman et al., 2012; Liu et al., 2014), but still higher than those expected with unaerated feeding (Fig. 5). Increasing the duration of an aerated feeding phase would improve the conversion efficiency further, as this approaches fully continuous operation more and more, as Mozo et al. (2012) illustrated for several volatile organics. However, granulation is hindered by aeration during the feeding phase (de Kreuk and van Loosdrecht, 2004). Therefore, this is not a viable strategy to improve the methane conversion in sequentially operated aerobic granular sludge reactors, as the environmental benefits of this technology would be lost, i.e. the lower energy, chemical and area requirements (Pronk et al., 2017). The development of aerobic granular sludge in a continuous flow reactor (Kent et al., 2018) may partly combine these benefits with a significant methane conversion efficiency, but the exact effect of the intragranule transport resistance is still uncertain (Fig. 8).

As methane consumption is expected to be limited, other strategies seem more effective to reduce methane emissions from sequentially operated reactors with unaerated feeding. First of all, methane production in the sewers can be minimized via appropriate design and/or chemical dosing (Liu et al., 2015; Terryn et al., 2017). The head-works can be covered and ventilated in case of a high influent methane and intense contact with air, so that the methane enriched ventilation air can be treated separately, for example in a biofilter (Huete et al., 2018). If the head-works do not significantly strip the influent methane, the succeeding reactors could be covered instead. The latter would be cheaper for aerobic granular sludge reactors due to their compactness. If anaerobic digestion is used, enclosed sludge treatment and storage units can limit emissions (Delre et al., 2017). Moreover, significant methane oxidation is expected if the methane-rich reject water is treated separately in a partial nitritation-anammox reactor (Castro-Barros et al., 2018). This is only effective in reducing plants-wide emissions if the reject water represents a significant fraction of the total liquid-phase methane entering the main stream, which is not always the case (Rodriguez-Caballero et al., 2014). This study indicates that also for partial nitritation-anammox reactors, continuous operation is preferred over sequential operation in this respect (Joss et al., 2009). Finally, valuable polymers can be extracted from waste aerobic granular sludge. This alternative sludge treatment would reduce the COD load to the digesters (Kehrein et al., 2020; Schaafsma et al., 2016), if present, and could therefore reduce methane emissions from this hot-spot.

It should be noted that the proposed mitigation strategies come at an environmental and economic cost. Further research is necessary to determine when the environmental benefit of avoiding the methane emissions in such a manner outweighs the environmental costs for the extra equipment and energy consumption. The answer will certainly depend on the specific plant, especially on the influent methane concentration. From the wide range of concentrations at the plant entrance (Table 1), a maximal emission between 0.5 and 15.3 g CH_4 is expected per m^3 of wastewater, assuming no methane oxidation and no anaerobic digesters. This corresponds to 0.017–0.520 kg $CO_2.m^{-3}$ on a 100-year time horizon (Myhre et al., 2013). Since the total carbon footprint of a wastewater treatment plant can easily vary between 0.6 and 1.7 kg $CO_2.m^{-3}$ (Maktabifard et al., 2020), the contribution of methane can be negligible in some cases (<0.1%) and substantial in others.

It should be noted that dedicated systems for methane removal with efficiencies of over 99% exist. For example, downflow hanging sponge reactors have been used for post-treatment of anaerobic effluent from UASB reactors (Matsuura et al., 2015; Matsuura et al., 2017). Their high methane removal efficiency can be explained by the continuous feeding and aeration (see Section 3.1.1), by the low influent COD concentrations which limit the competition from heterotrophs (see Section 3.2) and by the different liquid-gas transfer in such closed trickling filter systems. However, these systems are specifically designed as post-treatment of anaerobic effluents to remove methane and thus cannot be directly compared with aerobic granular sludge or activated sludge systems, which are designed to remove COD, nitrogen and phosphorus from wastewater directly.

4. Conclusion

Mathematical modeling was used to investigate the fate of methane entering sequentially operated aerobic granular sludge reactors.

- An unaerated feeding phase increased the methane concentration during aeration, which favoured stripping and lowered the conversion efficiency compared to a continuously operated reactor with simultaneous aeration and feeding.
- Even for a best-case scenario with an unrealistically low intragranule substrate transport resistance, a high retention time of methane oxidizing bacteria, a tall reactor, for an extremely high influent methane concentration and without considering oxygen limitation, the methane conversion efficiency was significantly lower (12%) than typical values measured in activated sludge reactors with simultaneous aeration and feeding (>48%). No conversion was predicted under more realistic assumptions and more moderate conditions.
- Mitigation of methane emissions from plants with sequentially operated reactors can be based on minimizing production in the

sewers, controlled stripping and separate treatment of the ventilation air and alternative sludge treatment.

Declaration of Competing Interest

The authors declare that they have no known competing financial interests or personal relationships that could have appeared to influence the work reported in this paper.

Acknowledgments

The doctoral research work of Janis Baeten has been financially supported by the Research Foundation Flanders (FWO) through a PhD fellowship. We thank Lenno van den Berg for his useful comments on the role of methane diffusion in granules.

Supplementary materials

Supplementary material associated with this article can be found, in the online version, at doi:10.1016/j.watres.2021.117619.

References

V. Abalakin (2010) Handbook of Chemistry and Physics. Haynes, W.M. (ed), pp. 14-13, Taylor & Francis, Boca Raton.
Ali, M., Wang, Z., Salam, K.W., Hari, R.A., Pronk, M., van Loosdrecht, M.C.M., Saikaly, P. E, 2019. Importance of species sorting and immigration on the bacterial assembly of different-sized aggregates in a full-scale aerobic granular sludge plant. Environ. Sci. Technol. 53 (14), 8291–8301.
Arcangeli, J.P., Arvin, E., 1999. Modeling the growth of a methanotrophic biofilm: estimation of parameters and variability. Biodegradation 10 (3), 177–191.
N. Artan and D. Orhon. (2005) Mechanism and Design of Sequencing Batch Reactors for Nutrient Removal, IWA publishing, London.
Baeten, J.E., Batstone, D.J., Schraa, O.J., van Loosdrecht, M.C.M., Volcke, E.I.P, 2019. Modeling anaerobic, aerobic and partial nitritation-anammox granular sludge reactors - a review. Water Res. 149, 322–341.
Baeten, J.E., van Dijk, E.J.H., Pronk, M., van Loosdrecht, M.C.M., Volcke, E.I.P., 2021. Potential of off-gas analyzes for sequentially operated reactors demonstrated on full-scale aerobic granular sludge technology. Science of The Total Environment 787, 147651.
Baeten, J.E., van Loosdrecht, M.C.M., Volcke, E.I.P, 2018. Modeling aerobic granular sludge reactors through apparent half-saturation coefficients. Water Res. 146, 134–145.
Baeten, J.E., van Loosdrecht, M.C.M., Volcke, E.I.P, 2020. When and why do gradients of the gas phase composition and pressure affect liquid-gas transfer? Water Res. 178, 115844.
Castro-Barros, C.M., Ho, L.T., Winkler, M.K.H., Volcke, E.I.P, 2018. Integration of methane removal in aerobic anammox-based granular sludge reactors. Environ. Technol. 39 (13), 1615–1625.
Çengel, Y.A., Cimbala, J.M., Turner, R.H., 2012. Fundamentals of Thermal-Fluid Sciences. McGraw-Hill.
Chen, X., Guo, J., Shi, Y., Hu, S., Yuan, Z., Ni, B.J, 2014. Modeling of simultaneous anaerobic methane and ammonium oxidation in a membrane biofilm reactor. Environ. Sci. Technol. 48 (16), 9540–9547.
Daebeler, A., Bodelier, P.L.E., Yan, Z., Hefting, M.M., Jia, Z.J., Laanbroek, H.J, 2014. Interactions between thaumarchaea, nitrospira and methanotrophs modulate autotrophic nitrification in volcanic grassland soil. ISME J. 8 (12), 2397–2410.
Daelman, M.R.J., Van Eynde, T., van Loosdrecht, M.C.M., Volcke, E.I.P, 2014. Effect of process design and operating parameters on aerobic methane oxidation in municipal WWTPs. Water Res. 66, 308–319.
Daelman, M.R.J., van Voorthuizen, E.M., van Dongen, U.G.J.M., Volcke, E.I.P., van Loosdrecht, M.C.M., 2012. Methane emission during municipal wastewater treatment. Water Res. 46 (11), 3657–3670.
de Bruin, L.M.M., de Bruin, B., van der Roest, H., van Bentem, A., Berkhof, D., van Dijk, E.J.H., van Gool, H., Kraan, R., Krijgsman, J., van der Kuij, R., van Loosdrecht, M.C.M., Meinema, K., Miska, V., Pronk, M., Verschoor, J., Winkler, M., 2013. Nereda Praktijkonderzoeken 2010–2012. STOWA, Amersfoort.
de Kreuk, M.K., van Loosdrecht, M., 2004. Selection of slow growing organisms as a means for improving aerobic granular sludge stability. Water Sci. Technol. 49 (11), 9–17.
Delre, A., Monster, J., Scheutz, C., 2017. Greenhouse gas emission quantification from wastewater treatment plants, using a tracer gas dispersion method. Sci. Total Environ. 605, 258–268.
Foley, J., Yuan, Z., Senante, E., Chandran, K., Willis, J., van Loosdrecht, M.C.M., van Voorthuizen, E.M., 2011. N_2O and CH_4 Emission From Wastewater Collection and Treatment Systems - State of the Science Report. Global Water Research Coalition.
Foley, J., Yuan, Z.G., Lant, P., 2009. Dissolved methane in rising main sewer systems: field measurements and simple model development for estimating greenhouse gas emissions. Water Sci. Technol. 60 (11), 2963–2971.
Gmehling, J., Menke, J., Krafczyk, J., Fischer, K., Fontaine, J.C., Kehiaian, H.V., Haynes, W.M., 2010. Handbook Of Chemistry And Physics. Taylor & Francis, Boca Raton, p. 247.
Hauduc, H., Rieger, L., Takacs, I., Heduit, A., Vanrolleghem, P.A., Gillot, S., 2010. A systematic approach for model verification: application on seven published activated sludge models. Water Science and Technology 61 (4), 825–839.
Henze, M., Gujer, W., Mino, T., van Loosdrecht, M.C.M., 2000. Activated sludge models ASM1, ASM2, ASM2d and ASM3. IWA Publishing, London, UK.
Henze, M., van Loosdrecht, M.C.M., Ekama, G.A., Brdjanovic, D., 2008. Biological Wastewater Treatment: Principles, Modeling and Design. IWA Publishing.
Huete, A., de los Cobos-Vasconcelos, D., Gómez-Borraz, T., Morgan-Sagastume, J.M., Noyola, A., 2018. Control of dissolved CH_4 in a municipal UASB reactor effluent by means of a desorption – biofiltration arrangement. J. Environ. Manag. 216, 383–391.
Jones, R.D., Morita, R.Y, 1983. Methane oxidation by nitrosococcus oceanus and nitrosomonas europaea. Appl. Environ. Microbiol. 45 (2), 401–410.
Joss, A., Salzgeber, D., Eugster, J., Konig, R., Rottermann, K., Burger, S., Fabijan, P., Leumann, S., Mohn, J., Siegrist, H., 2009. Full-scale nitrogen removal from digester liquid with partial nitritation and anammox in one SBR. Environ. Sci. Technol. 43 (14), 5301–5306.
Kehrein, P., van Loosdrecht, M., Osseweijer, P., Posada, J., 2020. Exploring resource recovery potentials for the aerobic granular sludge process by mass and energy balances - energy, biopolymer and phosphorous recovery from municipal wastewater. Environ. Sci. Water Res. Technol. 6 (8), 2164–2179.
Kent, T.R., Bott, C.B., Wang, Z.W, 2018. State of the art of aerobic granulation in continuous flow bioreactors. Biotechnol. Adv. 36 (4), 1139–1166.
King, G.M., Schnell, S., 1994. Ammonium and nitrite inhibition of methane oxidation by methylobacter albus BG8 and methylosinus trichosporium OB3b at low methane concentrations. Appl. Environ. Microbiol. 60 (10), 3508–3513.
Kuba, T., Smolders, G., van Loosdrecht, M.C.M., Heijnen, J.J, 1993. Biological phosphorus removal from waste-water by anaerobic-anoxic sequencing batch reactor. Water Sci. Technol. 27 (5-6), 241–252.
Kwok, C.E.Y., Muller, D., Caldow, C., Lebegue, B., Monster, J.G., Rella, C.W., Scheutz, C., Schmidt, M., Ramonet, M., Warneke, T., Broquet, G., Ciais, P., 2015. Methane emission estimates using chamber and tracer release experiments for a municipal waste water treatment plant. Atmos. Meas. Tech. 8 (7), 2853–2867.
Liu, Y., Cheng, X., Lun, X., Sun, D., 2014. CH_4 emission and conversion from A2O and SBR processes in full-scale wastewater treatment plants. J. Environ. Sci. 26 (1), 224–230.
Liu, Y., Ni, B.J., Sharma, K.R., Yuan, Z., 2015. Methane emission from sewers. Sci. Total Environ. 524-525, 40–51.
Lopes, F., Viollier, E., Thiam, A., Michard, G., Abril, G., Groleau, A., Prévot, F., Carrias, J. F., Albéric, P., Jézéquel, D., 2011. Biogeochemical modeling of anaerobic vs. aerobic methane oxidation in a meromictic crater lake (Lake Pavin, France). Appl. Geochem. 26 (12), 1919–1932.
Maktabifard, M., Zaborowska, E., Makinia, J., 2020. Energy neutrality versus carbon footprint minimization in municipal wastewater treatment plants. Bioresour. Technol. 300, 122647.
Masuda, S., Sano, I., Hojo, T., Li, Y.Y., Nishimura, O., 2018. The comparison of greenhouse gas emissions in sewage treatment plants with different treatment processes. Chemosphere 193, 581–590.
Masuda, S., Suzuki, S., Sano, I., Li, Y.Y., Nishimura, O., 2015. The seasonal variation of emission of greenhouse gases from a full-scale sewage treatment plant. Chemosphere 140, 167–173.
Matsuura, N., Hatamoto, M., Sumino, H., Syutsubo, K., Yamaguchi, T., Ohashi, A., 2015. Recovery and biological oxidation of dissolved methane in effluent from UASB treatment of municipal sewage using a two-stage closed downflow hanging sponge system. J. Environ. Manag. 151, 200–209.
Matsuura, N., Hatamoto, M., Yamaguchi, T., Ohashi, A., 2017. Methanotrophic community composition based on pmoA genes in dissolved methane recovery and biological oxidation closed downflow hanging sponge reactors. Biochem. Eng. J. 124, 138–144.
Meija, J., Coplen, T.B., Berglund, M., Brand, W.A., De Bievre, P., Groning, M., Holden, N. E., Irrgeher, J., Loss, R.D., Walczyk, T., Prohaska, T., 2016. Atomic weights of the elements 2013 (IUPAC technical report). Pure Appl. Chem. 88 (3), 265–291.
Mozo, I., Lesage, G., Yin, J., Bessiere, Y., Barna, L., Sperandio, M., 2012. Dynamic modeling of biodegradation and volatilization of hazardous aromatic substances in aerobic bioreactor. Water Res. 46 (16), 5327–5342.
G. Myhre, D. Shindell, F.M. Bréon, W. Collins, J. Fuglestvedt, J. Huang, D. Koch, J.F. Lamarque, D. Lee, B. Mendoza, T. Nakajima, A. Robock, G. Stephens, T. Takemura and H. Zhan 2013 Anthropogenic and Natural Radiative Forcing. Stocker, T.F., Qin, D., Plattner, G.K., Tignor, M., Allen, S.K., Boschung, J., Nauels, A., Xia, Y., Bex, V. and Midgle, P.M. (eds), Cambridge University Press, Cambridge, UK and New York, USA.
Nyerges, G., Stein, L.Y, 2009. Ammonia cometabolism and product inhibition vary considerably among species of methanotrophic bacteria. FEMS Microbiol. Lett. 297 (1), 131–136.
O'Neill, J.G., Wilkinson, J.F, 1977. Oxidation of ammonia by methane-oxidizing bacteria and the effects of ammonia on methane oxidation. Microbiology 100 (2), 407–412.
Pronk, M., de Kreuk, M.K., de Bruin, B., Kamminga, P., Kleerebezem, R., van Loosdrecht, M.C.M., 2015. Full scale performance of the aerobic granular sludge process for sewage treatment. Water Res. 84, 207–217.
Pronk, M., Giesen, A., Thompson, A., Robertson, S., van Loosdrecht, M., 2017. Aerobic granular biomass technology: advancements in design, applications and further developments. Water Pract. Technol. 12 (4), 987–996.
Reichert, P., 1994. AQUASIM – A tool for simulation and data analysis of aquatic systems. Water Science and Technology 30 (2), 21–30.

Ren, Y.G., Wang, J.H., Li, H.F., Zhang, J., Qi, P.Y., Hu, Z., 2013. Nitrous oxide and methane emissions from different treatment processes in full-scale municipal wastewater treatment plants. Environ. Technol. 34 (21), 2917–2927.
Ribera-Guardia, A., Bosch, L., Corominas, L., Pijuan, M., 2019. Nitrous oxide and methane emissions from a plug-flow full-scale bioreactor and assessment of its carbon footprint. J. Clean. Prod. 212, 162–172.
Rodriguez-Caballero, A., Aymerich, I., Poch, M., Pijuan, M., 2014. Evaluation of process conditions triggering emissions of green-house gases from a biological wastewater treatment system. Sci. Total Environ. 493, 384–391.
Roeleveld, P.J., van Loosdrecht, M.C.M., 2002. Experience with guidelines for wastewater characterisation in The Netherlands. Water Sci. Technol. 45 (6), 77–87.
Samuelsson, J., Delre, A., Tumlin, S., Hadi, S., Offerle, B., Scheutz, C., 2018. Optical technologies applied alongside on-site and remote approaches for climate gas emission quantification at a wastewater treatment plant. Water Res. 131, 299–309.
Sander, R., 2015. Compilation of Henry's law constants (version 4.0) for water as solvent. Atmos. Chem. Phys. 15 (8), 4399–4981.
Schaafsma, M., Westerhuijs, P., van Loosdrecht, M.C.M., 2016. Marktverkenning en haalbaarheidsstudie Nereda®-alginaat en -granulaat. STOWA, Amersfoort.
Short, M.D., Daikeler, A., Wallis, K., Peirson, W.L., Peters, G.M, 2017. Dissolved methane in the influent of three Australian wastewater treatment plants fed by gravity sewers. Sci. Total Environ. 599-600, 85–93.
Sin, G., Kaelin, D., Kampschreur, M.J., Takacs, I., Wett, B., Gernaey, K.V., Rieger, L., Siegrist, H., van Loosdrecht, M.C.M, 2008. Modeling nitrite in wastewater treatment systems: a discussion of different modeling concepts. Water Sci. Technol. 58 (6), 1155–1171.
Terryn, I.C.C., Cocarcea, A., Lazar, G., 2017. Mitigation of hazardous air pollutant emissions: vacuum vs. conventional sewer system. Environ. Eng. Manag. J. 16 (4), 809–819.
van Dijk, E.J.H., Pronk, M., van Loosdrecht, M.C.M., 2018. Controlling effluent suspended solids in the aerobic granular sludge process. Water Res. 147, 50–59.
Vanrolleghem, P.A., Insel, G., Petersen, B., Sin, G., De Pauw, D., Nopens, I., Dovermann, H., Weijers, S., Gernaey, K.V, 2003. A comprehensive model calibration procedure for activated sludge models. In: Proceedings of the Water Environment Federation, pp. 210–237.
Wang, J., Zhang, J., Xie, H., Qi, P., Ren, Y., Hu, Z., 2011. Methane emissions from a full-scale A/A/O wastewater treatment plant. Bioresour. Technol. 102 (9), 5479–5485.
Wanner, O., Gujer, W., 1986. A multispecies biofilm model. Biotechnology and Bioengineering 28 (3), 314–328.
Ward, B.B., 1987. Kinetic studies on ammonia and methane oxidation by nitrosococcus-oceanus. Arch. Microbiol. 147 (2), 126–133.
Wei, S.P., Stensel, H.D., Nguyen Quoc, B., Stahl, D.A., Huang, X., Lee, P.H., Winkler, M.K. H, 2020. Flocs in disguise? High granule abundance found in continuous-flow activated sludge treatment plants. Water Res. 179, 115865.
Winkler, M.K.H., Kleerebezem, R., Khunjar, W.O., de Bruin, B., van Loosdrecht, M.C.M., 2012. Evaluating the solid retention time of bacteria in flocculent and granular sludge. Water Res. 46 (16), 4973–4980.
Yoshida, H., Mønster, J., Scheutz, C., 2014. Plant-integrated measurement of greenhouse gas emissions from a municipal wastewater treatment plant. Water Res. 61, 108–118.
Yoshinari, T., 1985. Nitrite and nitrous oxide production by Methylosinus trichosporium. Can. J. Microbiol. 31 (2), 139–144.